Earthquake Engineering, Tenth World Conference © 1992 Balkema, Rotterdam. ISBN 90 5410 060 5

Dynamic behaviour of super deep vertical shaft during earthquake

N.Ohbo, K.Hayashi & K.Ueno
Kajima Technical Research Institute, Japan
Y.Kaneko
Japan Sewage Works Agency, Japan

ABSTRACT: In order to clarify the deformation of super-deep vertical structure due to earthquake, an earthquake observation is carried out at a super-deep vertical shaft with a circular cross-section having a 22 m outer diameter and 99 m depth. It was found that deformation of the EW component of the shaft is predominantly in the first vibration mode, and that of the NS component is predominantly in the second vibration mode. The difference between the deformations in the above-mentioned EW and NS horizontal components of the super-deep vertical shaft is mainly due to the connected shield tunnel direction.

1 INTRODUCTION

There is a great demand for a development of super-deep underground urban space in Metropolitan Tokyo area. In the Metropolitan Tokyo area, subway tubes and other underground structures are crisscrossed, therefore it is difficult to construct underground structures without interfering with such existing structures. Consequently it is necessary to construct the underground structure deeper than existing structure foundations and tunnels in the ground.

A construction technology of super-deep continuous underground wall has been developed to be applied to the earth retaining wall for large scale excavation and the wall thickens by a super-deep diaphragm wall method. In the near future, the construction of the super-deep vertical shaft as a starting shaft for a shield tunnel or ventilation of super-deep tunnel by using super-deep continuous underground wall will be increasing. However, a seismic response behavior of super-deep vertical structures is not made clear so far. Moreover, observed records of shafts during earthquakes are limited in number (Ohbo 1989, Kaizu 1990, Kato 1991).

The earthquake resistant design of underground structure was made by use of the seismic deformation method to compute stresses and strains on the structure due to a fundamental deformation of the surrounding ground during earthquakes. In super-deep underground structure such as a vertical shaft, the most important thing is to evaluate fundamental deformation of the surrounding ground.

However, the deformations of the super-deep shaft due to surrounding ground conditions and earthquake characteristics, such as seismic wave propagation of bed rock, epicentral distance, magnitude and frequency components, have not yet been sufficiently clarified.

In order to develop rational and economical earthquake-resistant design for super-deep vertical structure, it is necessary to understand seismic response behavior of the shafts. The purpose of this paper is to clarify the deformations of the super-deep shaft and surrounding ground caused by observed three earthquakes that have different epicentral distance.

2 OUTLINE OF SHAFT AND EARTHQUAKE OBSERVATION SYSTEM

The observation site is located in the east of the Metropolitan Tokyo area.

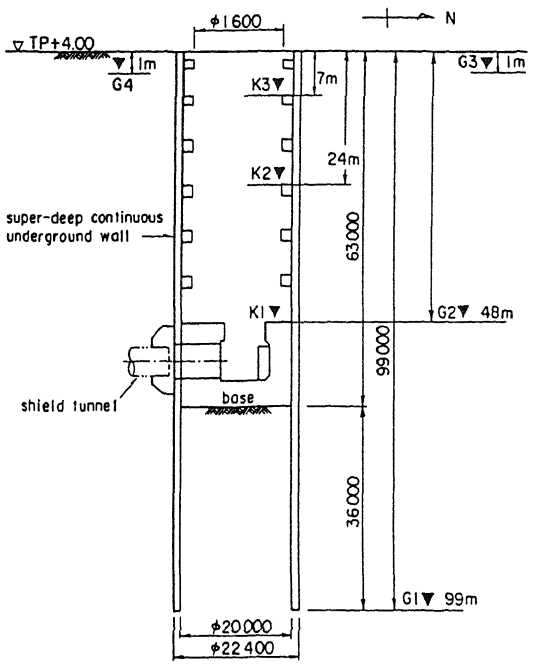

(a) Location of Instruments

Depth m	Name	H m	ρ t/m³	Vs m/s
-3.95	Alluvial sand	3.95	1.7	173
-23.10	Alluvial silt	19.15	1.6	153(I) 200(II)
-29.3	Alluvial silt	6.2	1.8	275
-34	Alluvial silt	4.7	1.9	245
-50.2	Alluvial sand	16.2	1.9	294
-67.6	Diluvial Clay	17.4	1.8	310
-78	Gravel	10.4	1.8	584(I) 600(II)
-99	Mudstone	21	1.8	584(I) 525(II)

(b) Soil Profile

Figure 1. Vertical section of the shaft, Location of Instruments and Soil Profile.

Figure 1 shows an NS directional vertical section of the super-deep vertical shaft with circular cross-section, soil profiles and location of instruments.

The shaft is super-deep continuous reinforced concrete underground wall, which was constructed by means of a diaphragm wall method incorporated with a slurry-assisted excavation method. The shield tunnel is at a depth of 50.8 m because it have to pass through under pile foundations of buildings. The depth of shaft is 99 m to shut off underground water into the shaft. The shaft has circular cross-section with outer diameter of 22 m and the thickness of the wall is 1.2 m

The surrounding soil layers consist of alluvial silts and sands, diluvial clay, gravel and mudstone from the ground level downward. The values of the shear wave velocity are assumed by using the relation between an N Value of standard penetration test and shear wave velocity. These values are in good correspondent to seismic wave propagation time delay from observed earthquake records.

As shown in Fig. 1 (a), seismographs were installed at three different depths (K1 ; GL-48m, K2 ; GL-24m and K3 ; GL-7m) inside the shaft as well as at four locations of surrounding ground. At surrounding ground : G1 at the toe of the shaft (GL-99m) ; G2 at GL-48m ; G3 and G4 at the depth of GL-1m 30m and 50m horizontally away from the center of the shaft respectively. Velocity servo seismographs, which provide high signal-to-noise ratios in the measurement of long-period components and three components, were used, and wave forms of velocity amplitudes have been being observed. Total number of components are 21 for velocity wave forms and 11 for acceleration wave forms mainly from the ground. These components are being observed simultaneously. The observation system uses telephone lines for reporting the outbreak of earthquakes and collecting earthquake data.

3 OBSERVED EARTHQUAKES

More than forty earthquakes have been observed since the installation of the instruments in December 1990. So far more than twenty-two earthquakes (seven of which had a maximum acceleration amplitude of 10 gal or

Table 1. Earthquake event Information and related data.

Event No.	Origin Time	M	Focal Depth (km)	Epicentral Distance (km)	Maximum Amplitude Acc(gal)	Maximum Amplitude Vel(kine)	I*
1	90:12:16	4.2	81	58	13.4	0.47	I
2	90:12:31	5.2	49	89	3.2	0.19	I
3	91:03:01	3.8	35	15	29.6	0.93	II
4	91:03:15	4.6	80	33	8.1	0.57	II
5	91:04:25	4.9	32	152	2.3	0.16	I
6	91:05:03	6.8	482	842	2.9	0.17	II
7	91:05:18	4.7	97	83	4.4	0.33	I
8	91:06:25	5.6	40	168	3.5	0.26	II
9	91:06:28	4.6	68	14	14.9	0.44	I
10	91:07:14	5.2	190	146	11.5	0.67	III
11	91:08:06	5.9	43	122	3.7	0.52	II
12	91:08:11	4.0	64	32	6.7	0.25	III
13	91:09:03	6.3	33	881	1.9	0.67	I
14	91:09:29	4.9	80	37	9.7	0.83	II
15	91:09:29	4.2	82	41	8.4	0.35	I
16	91:09:29	4.3	81	40	13.8	0.70	II
17	91:10:19	4.0	59	59	6.0	0.26	II
18	92:01:05	4.3	81	30	4.6	0.24	II
19	92:01:17	4.1	57	56	2.6	0.12	I
20	92:01:20	6.9	513	856	1.6	0.11	I
21	92:02:02	5.9	93	37	186.1	9.76	V
22	92:02:03	4.1	93	39	18.5	0.53	II

*: JMA Intensity at Tokyo

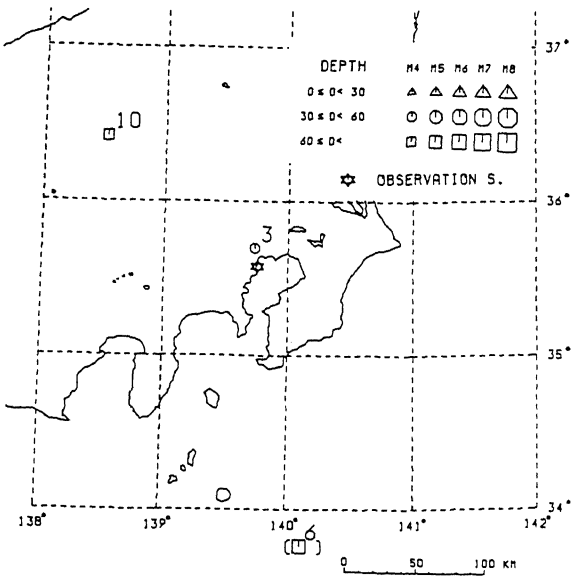

Figure 2. Location of epicenter and observation station.

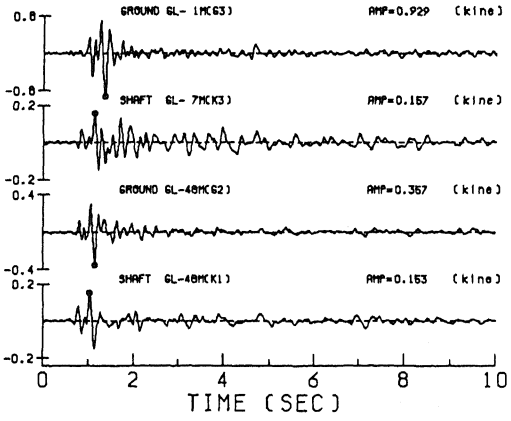

(a) Event No. 3 (epicentral distance 15km)

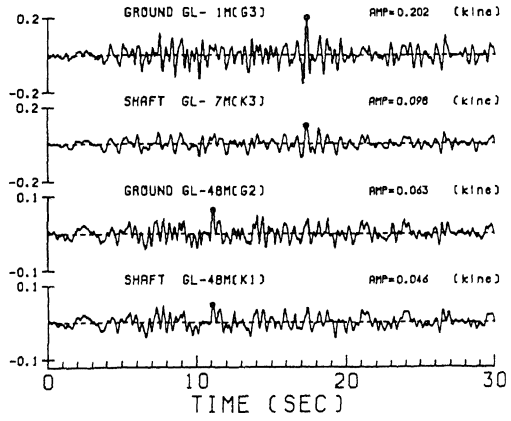

(b) Event No. 6 (epicentral distance 842 km)

Figure 3. Comparison of EW component Velocity time histories of the shaft and ground at the same depth (G3 and K3, G2 and K1).

more) with a maximum surface velocity amplitude of 0.1 kine (cm/sec) or more have been observed. Three of above-mentioned earthquakes with relatively larger magnitude and deference of epicentral distance, such as short epicentral distance (Event No.3 ; 15 km), middle (Event No.10 ; 146 km) and distant (Event No.6 ; 842 km), have been taken as examples. Table 1 summarizes a characteristic of earthquakes and maximum amplitudes of major earthquakes. Figure 2 shows the location of observation site and the epicenter of three earthquakes (Event No.3, No.6, and No.10) in Table 1. The location of epicenter of Event No.6 earthquake is out of the Fig. 2. So, the symbol indicating this Event is just showing the relative position to the earthquake wave propagation direction.

4 RESPONSE OF SHAFT AND FREE-FIELD SOIL

Figure 3 shows an example of recorded EW component velocity time histories at the ground (observation points G3 and G2) and in the

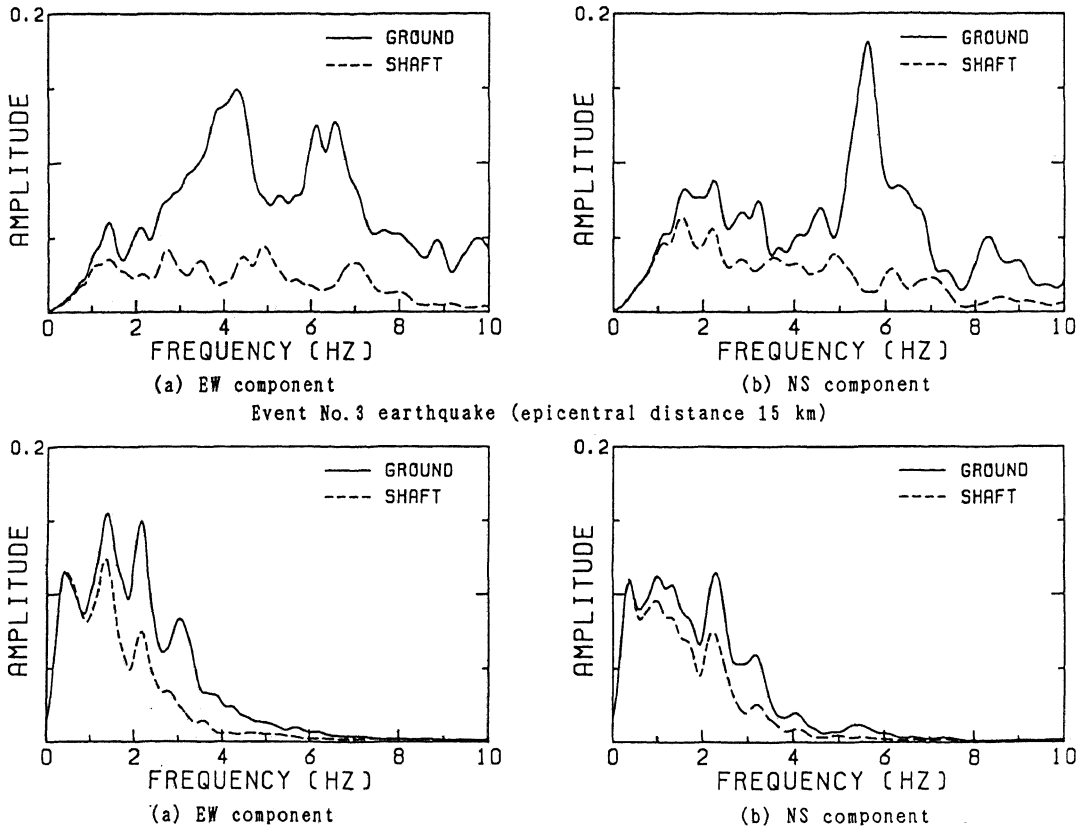

Figure 4. Comparison of Fourier spectra of the shaft (observation point K3) and the ground(observation point G3).

shaft (observation points K3 and K1) due to Event No. 3 and No. 6 earthquakes, respectively. Event No. 3 had the short epicentral distance whereas Event No. 6 had a distant one. In Event No. 3, a short period component can be seen and a duration is very short. Moreover, the amplitude of the shaft is smaller than that of the ground. On the other hand, in the response of the shaft and the ground for the distant earthquake Event No. 6, which have long period component and long duration, the time histories of the shaft and the ground are similar.

Figure 4 shows a superimposed Fourier spectra, which are obtained from the velocity time history of the horizontal component in the shaft (observation point K3) and on the ground (observation point G3) for Event No. 3 and No. 6, respectively. A solid line corresponds to the ground and the dash line corresponds to the shaft. Event No. 6 (see lower figure in Fig. 4) may be regarded as an example of a distant earthquake that usually contain considerably strong power in low frequency region. The Fourier spectrum in EW and NS components of the shaft and the ground are similar to each other. Moreover, peak frequencies of the shaft and the ground are almost the same. On the other hand, Event No. 3 (see upper figure of Fig. 4) shows a typical feature of the short epicentral distance. The NS component of the ground has a single dominant frequency at around 6 Hz, and EW component of the ground has two dominant frequencies at around 4 and 6 Hz. However, EW and NS components of the shaft have not so clear dominant frequency. It appears that the dominant frequency and amplitude of the ground due to the short distance earthquakes are different from those of the shaft. However, the responses of the ground and the shaft in the distant earthquake are almost the same.

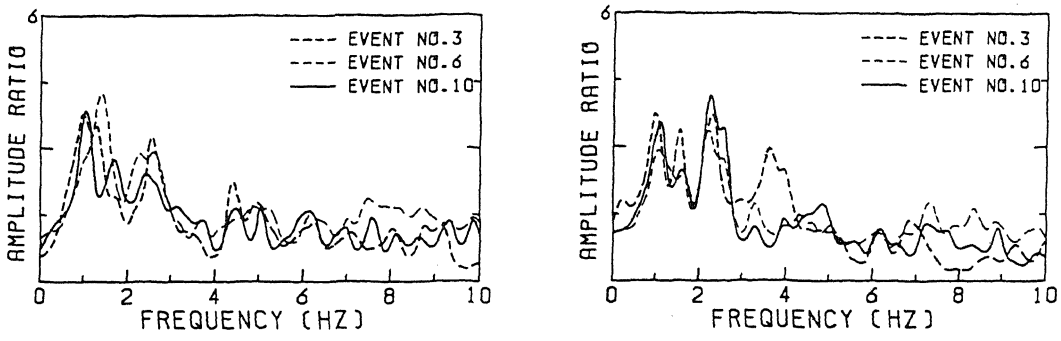

(a) EW component (b) NS component

Figure 5. Horizontal component frequency response function of K3/G1 for three earthquakes.

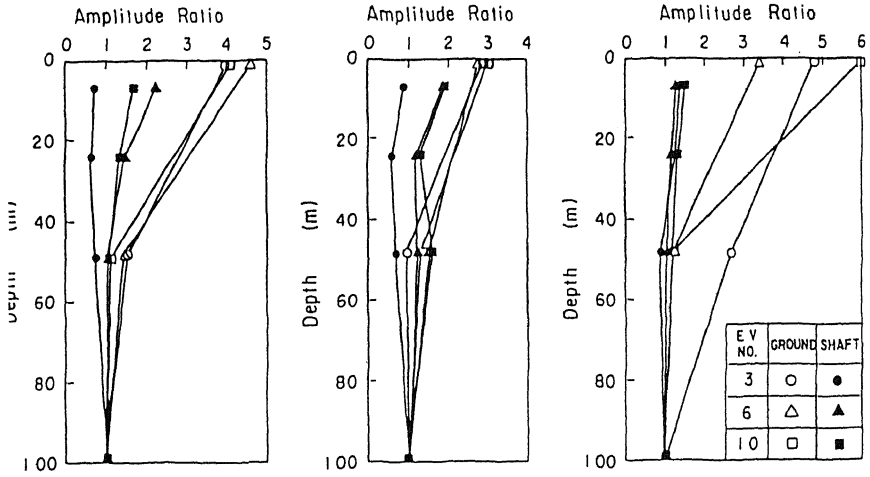

(a) EW component (b) NS component (c) UD component

Figure 6. Spatial distribution of maximum velocity amplitude ratio between shaft and ground for three earthquakes.

A vibration characteristic of the shaft can be recognized by frequency response function of the velocity at the top of the shaft with respect to input motion at the bottom. Figure 5 shows a superimposed frequency response function of the horizontal component at the top of the shaft, K3, corresponding to Fourier Spectra of input motion, G1, for three earthquakes Event No.3, No.6 and No.10, respectively. On the basis of Fig. 5, the vibration characteristics of the shaft during earthquakes with different epicentral distance have the dominant frequencies of 1.0 and 2.0 Hz in the EW component and NS component. The frequency around 1.0 Hz is most predominant in EW component, and the frequency around 2.0 Hz is predominant in the NS component. The frequency of 1.0 Hz corresponds to the fundamental vibration mode of the shaft, and that of NS component is around 2.0 Hz which corresponds to the second mode of the shaft. It seems that the difference between the predominant frequency of the shaft in EW and NS components depends on the connection of the shield tunnel direction.

Figure 6 shows a distribution of three components of a maximum velocity amplitude ratio for Event No.3, No.6 and No.10, respectively. The amplitude ratios at each observation point in the ground and the shaft correspond to the maximum amplitude of earthquake motion observed at point G1. The distribution of the amplitude ratio of horizontal component of the ground is independent of difference in epicentral distance of three earthquakes, and corresponds to the fundamental mode shape. On the contrary, UD component on the ground are different in distribution and amplification ratio depending on the three

earthquakes. The amplitude ratio of the shaft is smaller than that of the ground. EW component corresponds to the fundamental mode shape while NS component is different. This may be explained by the connecting of the shield tunnel to the shaft.

5. CONCLUSIONS AND REMARKS

Through the observation of the dynamic behavior of the super-deep vertical shaft and its surrounding ground due to earthquake, the deformation of the shaft was investigated. The results can be summarized as follows:

1. It is found that the dynamic behaviour of the shaft and ground are affected by the frequency content of the input motion.
2. The deformation of the shaft is strongly influenced by its being connected to the shield tunnel.

Based on the accumulated data obtained from seismic observation, the authors further investigate to the relationships between the magnitude of earthquakes and input earthquake motion as well as the behavior of the ground and shafts during earthquakes.

REFERENCES

Kaizu N., 1990, Seismic Response of Shaft for Underground Transmission Line, Proceedings from the Third Japan-U.S. Workshop on Earthquake Resistant Design of Lifeline Facilities and Countermeasures for Soil Liquefaction, 513-525.

Kato K., N. Ohbo, K. Hayashi & K. Ueno, 1991, Earthquake observation of Shaft and ground (in Japanese), Proceeding of the 46th Annual Conference of the JSCE, 1262-1261.

Ohbo, N., K. Hayashi & K. Ueno, 1989, Seismic Response of Shaft and shield Tunnel (in Japanese), Proceeding of the 44th Annual Conference of the JSCE, 1120-1121.